

RESEARCH

Open Access



# The brain reacting to COVID-19: analysis of the cerebrospinal fluid proteome, RNA and inflammation

Dirk Reinhold<sup>1,2†</sup>, Vadim Farztdinov<sup>3†</sup>, Yan Yan<sup>4,5†</sup>, Christian Meisel<sup>6</sup>, Henrik Sadlowski<sup>6</sup>, Joachim Kühn<sup>6</sup>, Frank H. Perschel<sup>6</sup>, Matthias Endres<sup>7,8</sup>, Emrah Düzel<sup>9</sup>, Stefan Vielhaber<sup>10</sup>, Karina Guttek<sup>1</sup>, Alexander Goihl<sup>1</sup>, Morten Venø<sup>5</sup>, Bianca Teegen<sup>11</sup>, Winfried Stöcker<sup>11</sup>, Paula Stubbemann<sup>12</sup>, Florian Kurth<sup>12</sup>, Leif E. Sander<sup>12</sup>, Markus Ralser<sup>3,15</sup>, Carolin Otto<sup>7</sup>, Simon Streit<sup>13</sup>, Sven Jarius<sup>14</sup>, Klemens Ruprecht<sup>7</sup>, Helena Radbruch<sup>13</sup>, Jørgen Kjems<sup>4</sup>, Michael Mülleler<sup>3</sup>, Frank Heppner<sup>13</sup> and Peter Körtvelyessy<sup>7,9,13\*</sup>

## Abstract

Patients with COVID-19 can have a variety of neurological symptoms, but the active involvement of central nervous system (CNS) in COVID-19 remains unclear. While routine cerebrospinal fluid (CSF) analyses in patients with neurological manifestations of COVID-19 generally show no or only mild inflammation, more detailed data on inflammatory mediators in the CSF of patients with COVID-19 are scarce. We studied the inflammatory response in paired CSF and serum samples of patients with COVID-19 ( $n = 38$ ). Patients with herpes simplex virus encephalitis (HSVE,  $n = 10$ ) and patients with non-inflammatory, non-neurodegenerative neurological diseases ( $n = 28$ ) served as controls. We used proteomics, enzyme-linked immunoassays, and semiquantitative cytokine arrays to characterize inflammatory proteins. Autoantibody screening was performed with cell-based assays and native tissue staining. RNA sequencing of long-non-coding RNA and circular RNA was done to study the transcriptome. Proteomics on single protein level and subsequent pathway analysis showed similar yet strongly attenuated inflammatory changes in the CSF of COVID-19 patients compared to HSVE patients with, e.g., downregulation of the apolipoproteins and extracellular matrix proteins. Protein upregulation of the complement system, the serpin proteins pathways, and other proteins including glycoproteins alpha-2 and alpha-1 acid. Importantly, calculation of interleukin-6, interleukin-16, and CXCL10 CSF/serum indices suggest that these inflammatory mediators reach the CSF from the systemic circulation, rather than being produced within the CNS. Antibody screening revealed no pathological levels of known neuronal autoantibodies. When stratifying COVID-19 patients into those with and without bacterial superinfection as indicated by elevated procalcitonin levels, inflammatory markers were significantly ( $p < 0.01$ ) higher in those with bacterial superinfection. RNA sequencing in the CSF revealed 101 linear RNAs comprising messenger RNAs, and two circRNAs being significantly differentially expressed in COVID-19 than in non-neuroinflammatory controls and neurodegenerative patients. Our findings may explain the absence of signs of intrathecal inflammation upon routine CSF testing despite the

<sup>†</sup>Dirk Reinhold, Vadim Farztdinov and Yan Yan contributed equally to this work.

\*Correspondence:

Peter Körtvelyessy

peter.koertvelyessy@charite.de

Full list of author information is available at the end of the article



presence of SARS-CoV2 infection-associated neurological symptoms. The relevance of blood-derived mediators of inflammation in the CSF for neurological COVID-19 and post-COVID-19 symptoms deserves further investigation.

**Keywords** COVID-19, Neuroinflammation, Proteomics, RNA, Progranulin

## Introduction

Infections with the severe acute respiratory syndrome coronavirus 2 (SARS-CoV-2) can result in a severe infectious syndrome requiring hospital admission and sometimes mechanical ventilation, which is sometimes accompanied by neurological manifestations such as headache, dys-/anosmia, encephalopathy and stroke (1–4). The evidence for direct brain damage due to SARS-CoV-2 infection is scarce and remains controversial (5, 6). Recently a preprint was published claiming that in ACE-2 mice, respiratory infection with SARS-CoV-2 is associated with damage to myelin and oligodendrocytes (7).

One major question is whether the neurological symptoms associated with coronavirus disease 2019 (COVID-19) are an indirect sequela of systemic SARS-CoV-2 infection, with the resulting cytokine storm reaching the CNS by passive diffusion or a leaky blood–brain barrier, or by a genuine intrathecal inflammatory response.

Until now SARS-CoV-2 has been detected with high-resolution microscopy only in the olfactory bulb and the peri-vascular regions in the medulla oblongata with known leaky blood brain barrier (5, 8, 9). Interestingly, microglial activation is prominent in most post-mortem studies of COVID-19 patients (5, 9), pointing at an at least passive reaction of the innate immunological system of the brain (8–10). Moreover, invading T cells in autopsy studies on patients with severe COVID-19 were described with a dominant activated effector phenotype from outside the CNS (11). On the other hand, except for evidence of mild-to-moderate blood–CSF barrier dysfunction, routine parameters in the CSF of patients with COVID-19 with or without additional neurological symptoms did not reveal any general signs of inflammation in the majority of patients (2, 3, 12–15). This result is in contrast to the findings in viral meningitis with very strong signs of inflammation in CSF such as high cell counts and increased protein content in CSF reflecting increased antibody synthesis in the brain. Also, the virus can be detected by PCR in the CSF, which until today could not be found without a doubt in infection with Sars-CoV 2. These signs of inflammation are not found in the CSF of COVID-19 patients (13).

Notably, the studies conducted so far did not distinguish between COVID-19 patients with and without a bacterial superinfection (BSI) distinguished by a procalcitonin level above 1 ng/ml as a sign of BSI or below. However, these superinfections, which occur most often

in severely affected patients with COVID-19, may also trigger an immunological response in the CNS biasing the immunological results.

We used a multi-omics approach together with ELISAs and antibody screening in an attempt to analyze and characterize neuro-inflammatory markers in the CSF/serum from COVID-19 patients. Our results point towards a mild but distinct response of the brain to peripheral inflammation rather than to an autochthonous intrathecal anti-viral immune response. Proteomic analyses showed a significant difference between COVID-19 patients with and without bacterial superinfections. By RNA sequencing, we found linear RNAs and circular RNAs that are dysregulated in the CSF of COVID-19 patients compared to healthy controls and patients with other neurological diseases.

## Materials and methods

### Demographic data and clinical features

This study has been approved by the ethics committee of the Charité Universitätsmedizin Berlin (EA176\_20). Every patient gave written and informed consent. We performed a retrospective study on CSF and serum samples from patients with PCR-proven SARS-CoV-2 infection in the nasopharyngeal area who underwent lumbar puncture to rule out CNS pathologies such as autoimmune encephalitis or meningitis involving a total of 38 COVID-19 patients. Classification according to the WHO definition resulted in 24 patients having grade 4 COVID-19, 7 patients with grade 3 COVID-19, 2 patients with grade one or two COVID-19, respectively. Three patients were SARS-CoV-2 positive as part of the general screening without showing any symptoms. The mean age of the patients was 68.6 years. 28 were male and 10 female. The indications for performing lumbar puncture were clinical symptoms of encephalopathy (dizziness, delirium, and headache) or prolonged awakening during the weaning. Specific neurological symptoms were very rare. One patient had myoclonia without signs of epilepsy on the EEG and one with oculomotor disturbances after resuscitation. Exclusion criteria were other neuroimmunological diseases such as other virus-meningitis, known history of multiple sclerosis (MS), or human immunodeficiency virus HIV. We defined two COVID-19 cohorts, one called Covid-19<sub>high PCT</sub> comprising COVID-19 patients having a procalcitonin (PCT) level above 1 ng/ml (cut-off

0.5 ng/ml) with levels ranging between 1.62 and 4.75 ng/ml (median = 3.85 ng/ml). We called the other COVID-19<sub>low PCT</sub> comprising COVID-19 patients with a PCT levels below 1 ng/ml, ranging between 0.03 and 0.94 ng/ml (median = 0.06 ng/ml). Procalcitonin is measured with an electro-chemo-luminescence-immuno-assay (Roche, Basel-Switzerland). We called the COVID-19<sub>high PCT</sub> also as bacterial superinfection (BSI) group.

We used for this study different group sizes of the control cohort ( $n=28$ ) and the Herpes-simplex virus meningoencephalitis (HSVE) cohort due to sample volume restrictions. We included 23 controls without a neurological diagnosis from the Charité biobank (ethical approval number EA4/018/17). The other 5 controls and 10 HSVE patients were recruited from the CSF lab at the Department of Neurology, Magdeburg (ethical approval number 07/17). These control patients received a spinal tap to exclude neurodegenerative, neuroimmunological diseases, or subarachnoid hemorrhage. None of these diagnoses has subsequently proven to be true. Every herpes simplex virus (HSV) patient had a positive HSV-PCR test in the CSF at diagnosis.

We used the data from other already existing control groups for cytokine, progranulin or RNA analysis. This collecting is approved by the local ethics committee of the university hospital Magdeburg (approval number (07/17)).

### Cytokine measurements

#### Cytokine array

For cytokine measurements, CSF and serum from 11 control patients and 10 patients with HSVE were used. We used a semi-quantitative neuroimmunology cytokine array (bio-technie, Minneapolis, MN) to analyze cytokine levels in CSF samples of COVID-19 patients ( $n=9$ ), HSVE patients ( $n=5$ ) and controls ( $n=4$ ) according to the manufacturer's instructions (16). This assay measures 36 human cytokines and inflammation-related proteins (CCL1, CCL2, MIP-1 $\alpha$ , CCL5, CD40L, C5/C5a, CXCL1, CXCL10, CXCL11, CXCL12, G-CSF, GM-CSF, ICAM-1, IFN- $\gamma$ , IL-1 $\alpha$ , IL-1 $\beta$ , IL-1ra, IL-2, IL-4, IL-5, IL-6, IL-8, IL-10, IL-12 p70, IL-13, IL-16, IL-17A, IL-17E, IL-18, IL-21, IL-27, IL-32 $\alpha$ , MIF, Serpin E1, TNF- $\alpha$ , TREM-1). We used the software Kodak D1 3.6 (Eastman Kodak, Rochester, New York), for determining the background-corrected sum intensity for each ROI on the membrane. Separate membranes were normalized to each other using the results of the positive controls.

#### ELISA measurements

The levels of IL-6, IL-16 and CXCL10 were measured in CSF samples and sera of 18 COVID-19 patients with mild-to-severe symptoms (12 COVID-19<sub>low PCT</sub> and 6

COVID-19<sub>high PCT</sub>), 10 HSVE patients and 11 normal controls using commercially available specific human Quantikine ELISA (bio-technie, Minneapolis, MN). The assays were performed following the instructions provided by the manufacturer.

### Progranulin measurements

We measured progranulin in the CSF of 21 COVID-19 patients (mean age 71.7 years, 6 female 15 male) with 12 belonging to the C19<sub>low PCT</sub> cohort and 9 to the C19<sub>high PCT</sub> cohort. Progranulin is differently metabolized in the CNS than outside the CNS and we, therefore, did not measure progranulin blood levels (17–19). Again, we used non-inflammatory, non-neurodegenerative controls ( $n=22$ ); receiving it now from the CSF lab at the Department of Neurology, university hospital Magdeburg. Progranulin measurements were done as described before with a commercial ELISA (20, 21).

### Autoantibody measurements

From 32 COVID-19 patients, CSF and serum samples were obtained at the same time and tested for anti-neuronal and anti-glial autoantibodies. Analysis was performed by Laboratory Prof. Dr. Stöcker (Lübeck, Germany,  $N=15$ ) and Labor Berlin (Berlin, Germany,  $N=19$ ). Every panel, in every laboratory, included antibodies to extracellular, synaptic, and intracellular epitopes. Two patients were measured in both laboratories, one with Yo-antibodies and one with NMDAR antibodies. At Labor Berlin, antibody screening in CSF/serum included testing for antibodies against NMDAR, LGI-1, Caspr2, DPPX, AMPAR, GABA<sub>B</sub>R, aquaporin-4, myelin, glycine receptor, dopamine-2R, mGluR5, GAD-65 using cell-based assays (CBA) and 12 paraneoplastic antibodies (anti-CV2, -Hu, -Ri, -Yo, -Ma2/Ta, -Zic4, -titin, -SOX1, -amphiphysin, -GAD65, -recoverin, Tr/DNER using immunoblots (Euroimmun, Germany). At the Laboratory Prof. Dr. Stöcker the same panel of 24 antibodies tested by Labor Berlin plus 12 additional antibodies (anti-CARPVIII, -mGluR1, -GABA<sub>A</sub>R, -ARH-GAP26/anti-Ca, ITPR1/anti-Sj, -Homer3, -Neurexin-3 alpha, -MOG, -neurochondrin, -IGLON-5, -flotillin-1 and -2) were measured by CBA. In addition, all serum and CSF samples at the Laboratory Prof. Dr. Stöcker were tested for novel autoantibody reactivities by immunohistochemistry on native hippocampus and cerebellum tissue sections on commercially available slides (Euroimmun, Lübeck).

### Mass spectrometry

#### Sample preparation

Cerebrospinal fluid (CSF) samples were reduced, alkylated, digested and conditioned on a Biomek i7

workstation, as previously described (22). Volumes and concentrations of reagents were adapted to accommodate the increased input volume. In short, 50  $\mu$ l CSF was transferred to 170  $\mu$ l 8 molar (M) urea, 5 mM DTT, 100 mM ABC buffer and incubated at 30 °C for 1 h before the addition of 18  $\mu$ l of 120 mM indole-3-acetic acid (IAA) and was incubated for 30 min at room temperature in the dark. 450  $\mu$ l of 100 mM ABC buffer was added, and 688  $\mu$ l of the solution was digested with 1.25  $\mu$ g trypsin in a total volume of 700  $\mu$ l and approx. 2 M Urea, at 37 °C over night. The reaction was stopped by the addition of 28  $\mu$ l 25% formic acid. 725  $\mu$ l of peptides were cleaned by solid phase extraction, vacuum dried and reconstituted in 50  $\mu$ l 0.1% formic acid and their concentration was determined (Pierce Quantitative Fluorometric Peptide Assay, number 23290).

### Mass spectrometry

Approximately 5  $\mu$ g of peptides (5  $\mu$ l) was used per injection for the 5-min gradient scanning SWATH LC-MS/MS (23). In brief, the peptides were resolved on an Agilent 1290 Infinity II system coupled to a TripleTOF 6600 mass spectrometer (SCIEX, Framingham, USA) equipped with IonDrive Turbo V Source (SCIEX). For reverse phase separation, we used a C18 ZORBAX rapid resolution high definition column (2.1 mm  $\times$  50 mm, 1.8  $\mu$ m particles) at a flow rate of 0.8 ml/min and column temperature of 30 °C. A linear gradient was applied which ramps from 1% B to 40% B in 5 min (Buffer A: 0.1% FA; Buffer B: ACN/0.1% FA) with a flow rate of 800  $\mu$ l/min. For washing the column, the organic solvent was increased to 80% B in 0.5 min and was kept for 0.2 min at this composition before going back to 1% B in 0.1 min. The column was equilibrated for 2.1 min before the next injection. The mass spectrometer was operated in high-sensitivity mode.

The data were recorded using scanning SWATH with a precursor isolation window of 10 m/z and a mass range of 400–900 m/z that was covered in 0.5 s. Nebulizer gas temperature, heater gas and curtain gas were set to 50 °C, 40 °C and 25 °C, respectively. The source temperature was set to 450 °C and the ion spray voltage to 5500 V. Raw data were binned in the quadrupole or precursor dimension into 8-m/z bins.

### Data processing

The raw data were processed using DIA-NN 1.7.12 (24) as previously described (22). MS2 and MS1 mass accuracies were set to 20 and 12 ppm, respectively, and scan window size set to 6. A spectral library was generated from a published list of peptides present in human CSF (PXD015087, 8250 peptides) (25) using the Deep learning-based spectra and RT prediction

provided in DIA-NN. The precursors were annotated using the Human UniProt sequence database (Human\_UP000005640\_9606, accessed 2019-12-20) (26). The library was automatically refined based on the dataset in question at 0.01 global q-value (using the “Generate spectral library” option in DIA-NN).

Peptide intensities, obtained after pre-treatment and annotation with DIA-NN, were subjected to quality control. Two samples with low quality were removed. Weighted mean scaling of intensities (with a weight proportional to the square of peptide presence and inversely proportional to its standard deviation) was applied to align sample intensity distributions within each group. Peptides with excessive missing values (>35% per group) were excluded from the analysis. To the rest of the peptides group-based imputation of missing values using a PCA method (27) was applied. Then they were normalized using LIMMA (28) implementation of cyclic loess method (29) with option “fast” (30). To obtain a quantitative protein data matrix, the log<sub>2</sub>-intensities of peptides were filtered and only peptides belonging to one protein group were kept and then summarized by “maxLFQ” method (31), implemented in R package iq (32), into protein log intensity. Median scaling of protein intensities was applied. Change of the data matrix after selected pre-processing steps is presented in Additional file 1: Table S3. A description of sample groups along with some demographic information is provided in Additional file 1: Table S4.

### Data analysis

The goals were (1) to find similarities/dissimilarities in the response to COVID-19 and HSVE meningitis and (2) to reveal the influence of bacterial superinfection on the neuroimmunological response. Statistical analysis of proteomics data was carried out using R scripts based on publicly available packages. Linear modeling was based on the R package LIMMA (28). Two models were applied to the data set.

Model 1:  $\log_2(p) \sim 0 + \text{Class}$ . Here,  $\log_2(p)$  is log<sub>2</sub> transformed expression of a protein. The categorical factor Class has four levels: control, C19\_low, C19\_high, HSVE; a reference level as control. The contrasts evaluated within Model 1 are listed in Table 2.

For finding regulated features the following criteria were applied:

Significance level alpha was set to guarantee the false discovery rate below ~5% across all contrasts. We found that  $\alpha = 0.01$  was delivering the required level of Benjamini–Hochberg FDR (33).

The log fold change criterion was applied to guarantee that the measured signal is above the average noise level. As such, we have taken median residual standard

deviation of the model:  $\log_2(T) = \text{median residual SD}$  of linear modeling.

Another set of selection criteria was applied for the creation of heatmaps. We applied very strict criteria:  $\alpha = 0.001$  was delivering Benjamini–Hochberg false discovery rate (FDR) below 1% and  $\log_2(T) = 1.5 \times \text{median residual SD}$ .

Model 1 allowed us to address the differences between clinical groups. Note that control and HSVE groups were confounded with gender and age (see Tab Change matrix) and this limits the accuracy of our findings.

Model 2:  $\log_2(p) \sim 0 + \text{sex} + f_2 + f_3$ .

The categorical factor sex has two levels: female and male; the reference level is male and factor  $f_2$  takes into account PCT level and  $f_3$  differences in the WHO grade.

Model 2 was devoted to a more accurate evaluation of the influence of bacterial superinfection on the proteome of COVID patients. For this, we used transformed numerical values of PCT levels  $f_2 = \log_2(1 + PCT)$ . As COVID-19 groups had roughly the same proportion of females ( $\sim 0.2$ ), sex was introduced into the model as a categorical factor. COVID-19 patients were of different WHO grades, which was confounded with PCT levels, therefore, to minimize its influence on the effect of BSI it was included into the model as a numerical factor  $f_3$ . Exploratory analysis revealed that the effect of age was relatively small and therefore was skipped from the analysis.

For model 2, the significance level alpha was set to guarantee the false discovery rate below  $\sim 10\%$  for contrast  $f_2$ . We found that  $\alpha = 0.01$  was delivering the required level of Benjamini–Hochberg FDR. The log fold change threshold was set as 0.5.

#### **Functional analysis of proteomics data**

Functional analysis (GSEA) was carried out using R package clusterProfiler. For selecting the most (de)regulated GO terms we applied filter:  $2 \leq \text{term size} \leq 250$ . Analyses were carried out with Benjamini–Hochberg FDR threshold of 0.3.

#### **The RNA sequencing of CSF and data analysis**

##### **Epidemiology of the long-noncoding RNA cohorts**

In the RNA sequencing, we used the CSF of 5 COVID-19 patients and 4 CSF samples from the control cohort. For comparison with other neurological diseases, we used an already established RNA data set of neurological diseases cohort (nd-cohort) at the Kjems' lab at the Department of Molecular Biology and Genetics at Aarhus University, Denmark. This nd cohort comprises 4 patients with

multiple sclerosis at diagnosis and 4 with AD (ethical approval number 07/17).

##### **CSF RNA purification and genomic DNA removal**

CSF samples were thawed in a cold room (4 °C) and then centrifuged at 5000 g 4 °C for 10 min. The supernatant was taken out for RNA purification.

For total RNA sequencing, 1 ml CSF was used for RNA purification using miRNeasy Serum/Plasma advanced kit (QIAGEN, Venlo, Netherlands) according to the manufacturer's protocol and the RNA was eluted in 50  $\mu$ l RNase-free water. The genomic DNA removal was done by using Turbo DNA-free kit (Ambion, MA, USA) according to the manufacturer's instructions and 50  $\mu$ l DNA-free RNA was taken out. The RNA was concentrated by adding 50  $\mu$ l RNase-free water, 10  $\mu$ l 3 M, pH 5.5 sodium acetate, 250  $\mu$ l pre-chilled 99% ethanol and 1  $\mu$ l Glycoblue (Ambion, MA, USA), and incubating at  $-20$  °C overnight. RNA was pelleted by centrifugation at 16,000 g for 20 min at 4 °C and the pellet was washed using 1 ml 80% ethanol. The RNA was re-pelleted by centrifugation at 10,000 g for 5 min and the RNA pellet was re-suspended in 12  $\mu$ l RNase-free water. The RNA was stored at  $-80$  °C.

##### **Total RNA sequencing**

The total RNA sequencing library was constructed by using 8  $\mu$ l of the RNA purified from 1 ml CSF and SMARTer Stranded Total RNA-Seq Kit v2—Pico Input Mammalian (Takara, Japan). The fragmentation time was 90 s and the rest of the experiment followed the protocol designed for the 250 pg RNA input. The Bioanalyzer High sensitivity DNA analysis kit (Agilent) was used to determine the size of the library fragments and the KAPA Library Quantification kit (Roche) was used to quantify the library. The libraries were pooled with an equal amount and sequenced on a Novaseq sequencing machine using SP flowcell paired-end 100 cycles (Illumina, MA, USA).

##### **Total RNA sequencing data analysis**

Sequencing data were pre-processed by removing the adapter sequence and trimming away low-quality bases with a Phred score below 20 using Trim Galore (v0.4.1). Quality control was performed using FastQC to ensure high-quality data. Quantification of gene expression was performed by mapping the filtered reads to the human genome (hg19) using Tophat2. The software featureCounts was used to quantify the number of reads mapping to each gene using gene annotation from the Gencode release 29. The linear RNAs were included in the further analysis if they had expression in all the



samples of at least one group (COVID-19 group, Healthy group or Neurological disease group). Quantification of circRNA was done primarily using CIRI2 and secondarily using find\_circ to support circRNA findings. Using bedtools detected circRNAs were checked against identical circRNAs annotated in circBase (PMID: 25234927), CIRCpedia (PMID: 30172046) and circAtlas (PMID: 32345360).

Differential expression analysis was performed using DESeq2 in R on the combined gene and circRNA expression levels. Volcano plots, dot plots and PCA plots were done in R. The linear RNA and circRNAs were considered to be significantly differentially expressed with the  $FDR < 0.05$ . The enrichment analysis was done using Enrichr (<https://maayanlab.cloud/Enrichr/>) (34). Every statistical method used is described under each subheading.

## Results

### Routine parameters in the COVID-19 cohort have an almost normal pattern

We studied CSF/serum pairs of a total of 38 patients with COVID-19. Ten patients with HSVE and 28 patients with non-inflammatory and non-neurodegenerative diseases served as controls. Demographic findings and the CSF parameters of patients and controls are summarized in Table 1. Consistent with previous findings (13, 14), routine CSF parameters of patients with COVID-19 showed normal levels with only the albumin CSF/serum ratio (median 10.24, range 5–43.6, normal ratios are from 4 to 9 increasing linearly with age) being slightly higher than normal (Table 1).

### CSF proteomics shows a mostly similar but attenuated inflammatory response in patients with COVID-19 as compared to HSVE

We used mass spectrometry to comprehensively analyze the CSF proteome in patients with COVID-19 as compared to patients with HSVE. Comparing the activated proteins in COVID-19 and HSVE show almost similar activation patterns but differences in both protein level

and regulation as seen with the direct comparison of regulated proteins in both cohorts (Fig. 1A, contrasts III and IV, see Table 2 for contrast overview). Several proteins are regulated in response to COVID-19 in either stronger or different directions than in HSVE. We found a large group of immunoglobulins and most of the complement components among proteins showing a similar but very attenuated response in COVID-19. Proteomics revealed a downregulation (in opposite to HSVE direction) of apolipoproteins APOA1, APOA2, APOA4 and APOC1; also an equal or stronger downregulation of CACNA2D1, NPTXR, NRCAM, NRXN2, SEMA7A, SIRPA, SLITR1 and VGF proteins (full list of protein abbreviations Additional file 1: Table S1). On the other hand, we could detect a stronger upregulation in COVID-19 of complement proteins C9, CFD, fibrinogen proteins FGA, FGB, FGG and some other proteins (AMBP, ITIH4, leucine-rich alpha-2-glycoprotein LRG1, alpha-1-acid glycoproteins ORM1, ORM2, SERPINA1, SERPINA3, SERPINF2, SERPING1, SGCE, PROCR, RBP4). A different protein upregulation than HSVE was detected for insulin-like growth factor-binding proteins IGFBP2, IGFBP4 and IGFBP6.

Taking into account immunosuppressive treatment with dexamethasone with a dosage ranging from 6 mg p.o. up to 100 mg i.v., no change was seen in the proteomics and the pathway analysis between the subgroup of COVID-19 patients treated ( $n=4$ ) versus the subgroup not treated ( $n=34$ ). The same result was already in the proteomics data of plasma from COVID-19 patients (22).

### Bacterial superinfection, as inferred from high PCT levels, aggravates the host response

Many proteins and the response protein pattern in COVID-19 patients with BSI and COVID-19 patients without BSI (contrast: COVID-19<sub>high PCT</sub> vs. COVID-19<sub>low PCT</sub>) are differently regulated compared to controls (contrast: COVID-19<sub>high PCT</sub> + COVID-19<sub>low PCT</sub> vs. controls). Similarly, the response protein pattern in

**Table 1** Epidemiological data and routine CSF results from the entire COVID-19 cohort, the HSVE cohort, and the proteomics controls

Parameter (normal value)	Covid 19	HSVE	Controls
Number	38	10	28
Sex (f:m)	10:28	6:4	17:11
Age	69.1 (29–88)	54.6 (24–91)	58.7 (39–82)
Cell count (4 <)	2.15 (0–23)	186.8 (22–514)	1.6 (0–5)
Protein [mg/dl]	487.3 (187–2404)	767.9 (326–1240)	362.9 (195.4–635.0)
Lactate (19 <) [mg/dl]	19.78	26.3 (19–32)	15.1 (9.0–18.1)
Albumin ratio (4–9)	10.24 (5–43.6)	15.5 (10.8–32.5)	n.a

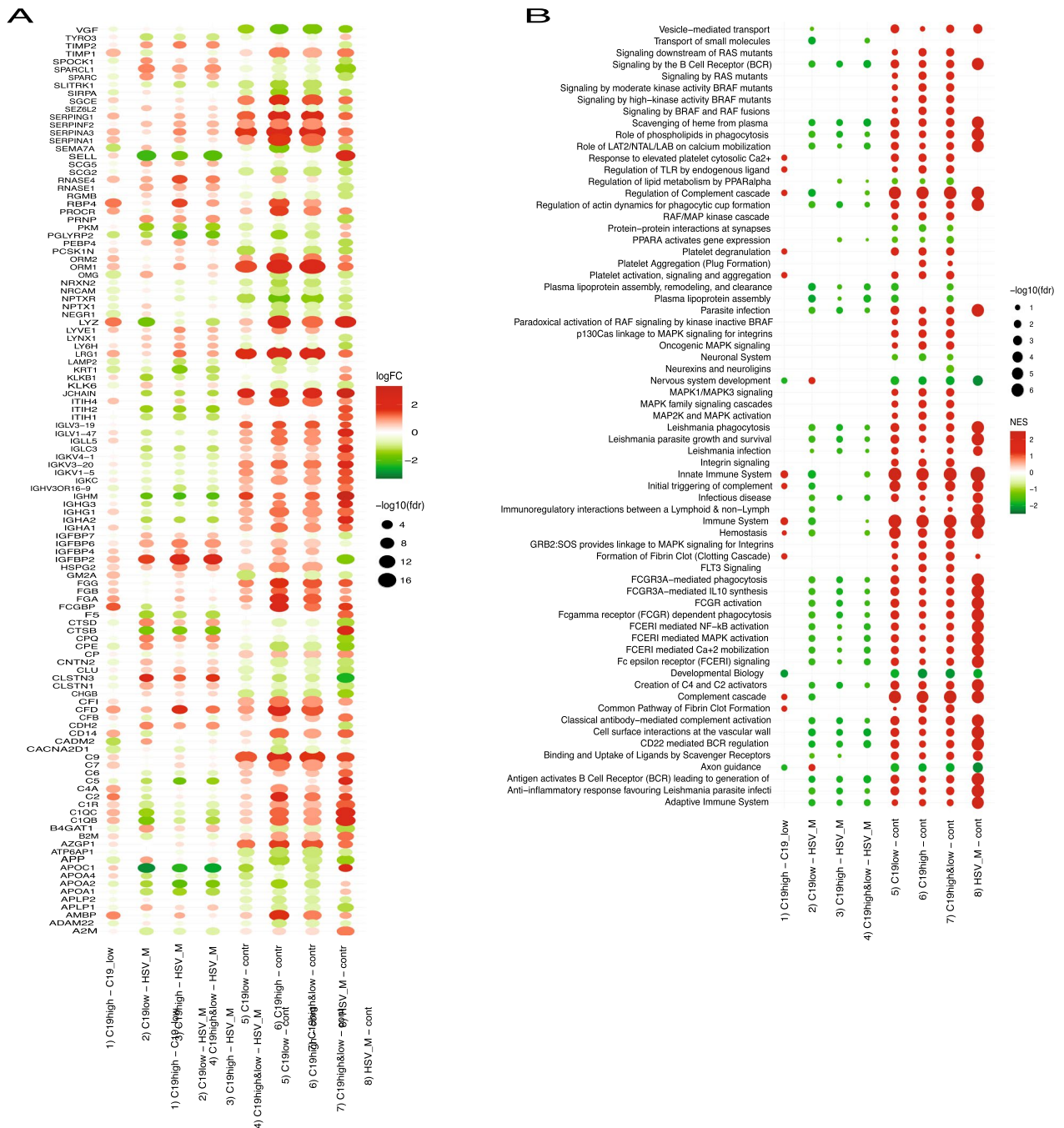


**Fig. 1** Proteomics analysis. **A** Dot heatmap of significantly regulated proteins across all contrasts. The proteins satisfy selection criteria:  $\alpha = 0.001$  and  $|\log_{2}FC| > 1$  at least in one of the eight contrasts (see Table 1), here shown as x-axis labels. All contrasts in this and the next plot are split into four groups: group I for comparison of C19 high PCT vs. C19 low PCT, group II for comparison of C19 groups vs. HSVE, group III for comparison of C19 groups vs. controls and group IV for comparison of HSVE group vs. controls. One can see that the strongest regulation (by the number of proteins with high  $|\log_{2}FC|$ ) is observed for HSVE vs. control (group IV). Regulation in a group of contrasts III (COVID-19 groups vs. control, contrasts 5–7 in Table 1) appears as following the regulation in group IV (contrast 8 in Table X2). Still, the extent of the regulation is different, as can be seen from the pattern of protein regulation in a group of contrasts II (COVID-19 groups vs. HSVE, contrasts 2–4 in Table 1). **B** Dot heatmap of significantly enriched REACTOME terms across all contrasts. Results of GSEA using REACTOME functional terms with  $FDR < 0.05$  at least in one of the eight contrasts (see Table 1). All contrasts in the plot are split into four groups: group I for comparison of C19 high PCT vs. C19 low PCT, group II for the comparison of C19 groups vs. HSVE, group III for the comparison of C19 groups vs. controls and group IV for the comparison of HSVE group vs. controls

**Table 2** Contrasts addressed in the Model 1 analysis

Contrast	Description	Short notation
Contrast 1	C19_high_PCT vs. C19_low_PCT	C19H/C19L
Contrast 2	C19_low_PCT vs. HSV meningoencephalitis	C19L/HSVE
Contrast 3	C19_high_PCT vs. HSV meningoencephalitis	C19H/HSVE
Contrast 4	(C19_low_PCT + C19_high_PCT)/2 vs. HSV meningoencephalitis	C19H&L/HSVE
Contrast 5	C19_low_PCT vs. control	C19L/cont
Contrast 6	C19_high_PCT vs. control	C19H/cont
Contrast 7	(C19_low_PCT + C19_high_PCT)/2 vs. control	C19H&L/cont
Contrast 8	HSV meningoencephalitis vs. control	HSVE/cont

C19 = COVID-19, C19H = COVID-19 with high PCT, C19L = COVID-19 with low PCT, HSVE = HSV meningoencephalitis

COVID-19 patients with BSI (COVID-19<sub>high PCT</sub> vs. controls) is highly correlated ( $\rho=0.94$ ) to the response in COVID-19 patients without BSI (COVID-19<sub>low PCT</sub> vs. controls).

When analyzing the response of proteins in COVID-19 patients with BSI compared to COVID-19 patients without BSI some proteins show a monotonic increase of response with the increase of  $\log_2(1+PCT)$ . Combined  $\log_2$  expression of the three proteins C4a, CD14 and NRCAM ( $y = (C4A + CD14)/2 - NRCAM$ ) used in a simple linear fit conducted on all COVID-19 samples resulted in dependence with a rather high coefficient of determination,  $R^2 = 0.67$  (see Additional file 1: Figure S1), meaning that these distinct proteins and their pathways are only activated in COVID-19 with BSI.

The comparisons of CSF proteomics from HSVE patients with controls show an overwhelming activation at almost every level in HSVE patients (Fig. 1B). Comparing the COVID-19 cohort to the same non-inflammatory controls reveals an almost similar protein activation pattern as the proteomics pattern in HSVE but on a much lower level in COVID-19 patients.

In total, more pathways were activated in the CSF proteomics of COVID-19 patients as in HSVE patients (Fig. 1B). The pathways connected with lipoproteins and nervous system development are especially enriched and downregulated, whereas the pathways connected with integrins, and fibrin clot formation are enriched and upregulated (Fig. 1B).

### Cytokine indices reveal no intrathecal production of cytokines

For a general assessment of the inflammatory response, 36 cytokines were measured in the CSF samples of COVID-19 ( $n=9$ ), HSVE ( $n=5$ ) and non-inflammatory,

non-neurodegenerative controls ( $n=4$ ) with a semiquantitative array technique via a background-corrected sum intensity analysis as described before (16). The analysis yielded a plethora of different elevated cytokine levels compared to controls (Fig. 2). Mean levels of CCL1, CXCL10, IL-1ra, IL-6, IL-8 and IL-16 as well as Serpin E1 and C5/C5a are elevated in the CSF of COVID-19 patients compared to non-neurological controls. Patients suffering from the severe neuroinflammatory disease HSVE had in general higher cytokine levels than any other disease. Only the level of IL-16 was higher in COVID-19 patients CSF than in HSVE patients with every other cytokine level being higher in the CSF of HSVE patients. We, therefore, excluded HSVE in general from statistics and used it only as a reference for cytokine ratios and proteomics in neuroinflammatory diseases.

We further examined CXCL10, IL-6 and IL-16, with specific ELISA (see Tables 3 and 4 and Fig. 3). This enabled us to calculate ratios between CSF and serum to determine the origin of each measured cytokine. Cerebrospinal fluid/serum ratios under 1 indicate a higher serum level. Non-neurological controls showed mean IL-6 concentrations of 3.2 pg/ml (range 0.5–9.7 pg/ml) in the CSF and 2.6 pg/ml (range 0–9.4 pg/ml) in the serum resulting in a CSF/serum IL-6 ratio of 1.2. Mean IL-6 levels as in the CSF of C19<sub>total</sub> patients was 37.0 pg/ml (range 0.7–552.1 pg/ml) and in serum 92.5 pg/ml (range 0.7–552.43 pg/ml) (Table 2 and Fig. 3A). Every IL-6 CSF/serum ratio in every COVID-19 patient was between 0.15–0.55 indicating an IL-6 origin from blood invading the CSF compartment. Patients with COVID-19 and low PCT had much lower mean IL-6 levels in the CSF [7.0 pg/ml, (range 0.7–24.7 pg/ml)] and serum [51.3 pg/ml (0.75–345.5 pg/ml)] than patients with COVID-19 and high PCT (IL-6 serum 174.9 pg/ml (7.1–552.4 pg/ml) and CSF with mean IL-6 levels at 96.9 pg/ml (range 1.5–552.1 pg/ml). Serum IL-6 levels in the C19<sub>high PCT</sub> patients compared to our non-neurological cohort were significantly higher ( $p < 0.01$ ). Significant differences ( $p < 0.05$ ) between IL-6 levels in the C19<sub>high PCT</sub> cohort and the C19<sub>low PCT</sub> cohort were found in the CSF but not between serum and CSF IL-6 levels, nor ratios. These results are in contrast to HSVE patients with a mean IL-6 concentration in CSF of 315.5 pg/ml (range 1.77–552.9 pg/ml) and serum of 12.7 pg/ml (range 0.3–573.3 pg/ml) resulting in a mean ratio of 24.84, pointing at the CNS as IL-6 source (see Table 4). In summary, CSF IL-6 levels are very likely driven by the serum IL-6 levels in COVID-19 patients.

IL-16 levels in CSF and serum were significantly higher in every COVID-19 patient than in non-neurological controls (see Table 3 for results and Fig. 3B). Significant differences were found in IL-16 concentrations in the serum between the C19<sub>low PCT</sub> cohort and C19<sub>high</sub>



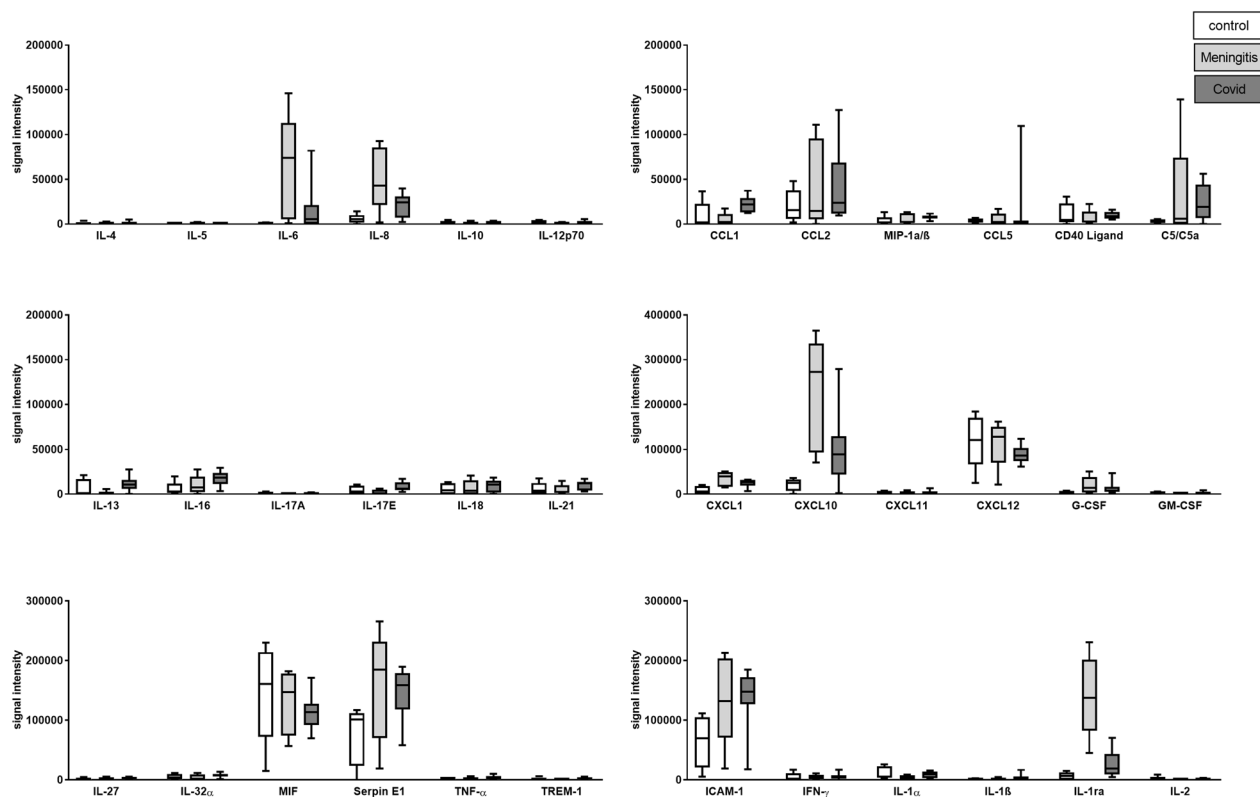


**Fig. 2** Results of the semi-quantitative cytokine arrays as box-plot

$P_{CT}$  cohort ( $p < 0.02$ ) but not in CSF ( $p = 0.48$ ) with serum IL-16 levels in the  $C19_{low}$   $P_{CT}$  cohort reaching a mean = 295 pg/ml (range 109.7–521.2 pg/ml) and in the  $C19_{high}$   $P_{CT}$  cohort with a mean = 486.6 pg/ml (ranging from 226.2 to 775.8 pg/ml). Every CSF/serum ratio for IL-16 was between 0.11 and 0.46 showing an origin from outside the CNS. This ratio turned significant when comparing IL-16 ratios from non-neurological controls with a highly inflammatory condition such as the  $C19_{high}$   $P_{CT}$  cohort ( $p < 0.01$ ) (Table 4).

CXCL10 levels in the serum of the  $C19_{Total}$  cohort (serum = 405.2 pg/ml, range 32.8–1234.3 pg/ml) are significantly higher ( $p < 0.05$ ) as in non-neurological controls (serum = 161.6 pg/ml, range 91.4–368.4 pg/ml) (Fig. 4C). In general, CXCL10 levels in the serum were higher than in the CSF for the entire COVID-19 cohort (serum = 405.2 pg/ml, 32.8–234.3 pg/ml versus CSF = 226.7 pg/ml, 49.1–622.1 pg/ml) resulting in CSF/serum ratios in between 0.53–0.59 pointing at a cytokine origin from outside of the CNS.

#### Progranulin levels point to microglial activation or lesions in the olfactory system

Progranulin is an anti-inflammatory protein produced by activated microglia and neurons throughout the brain

with the highest neuronal concentrations detected in the olfactory and temporal regions of the brain (35–37). The mean progranulin concentration in the total COVID-19 cohort was 1.68 ng/ml (range 0.67–3.04 ng/ml). This was significantly higher than in non-inflammatory, non-neurodegenerative controls (mean 1.00 ng/ml, range 0.49–2.09 ng/ml) ( $p < 0.01$ ) (Fig. 4D).

No significant difference in progranulin levels was found between the  $C19_{low}$   $P_{CT}$  (mean 1.68 ng/ml, range 0.67–3.04 ng/ml) subgroup and the  $C19_{high}$   $P_{CT}$  subgroup (mean 1.67 ng/ml, range 0.75–2.58 ng/ml). Three asymptomatic COVID-19 patients in whom the infection with SARS-CoV2 was accidentally found at hospital admission had normal progranulin levels in the CSF (mean 1.19 ng/ml, range 1.03–1.42 ng/ml). HSVE patients had the highest progranulin CSF levels (5.67 ng/ml, range 1.04–11.91 ng/ml) significantly higher than any other cohort.

#### Low-titer anti-neuronal antibodies in some patients but no evidence for autoimmune encephalitis

Three out of 32 patients were positive for serum anti-myelin IgG antibodies in a tissue-based assay. As a limitation, such antibodies have been observed also in other diseases and even in healthy controls and may thus be unspecific. In two patients, serum IgG antibodies against

**Table 3** Cytokine and progranulin levels and ratios in our groups

	N	Mean serum level (pg/mg)	Range (pg/ml)	Mean CSF level (pg/ml)	Range (pg/ml)	Ratio	Range
<i>IL-6</i>							
NC	11	2.6	0.0–9.4	3.2	0.5–9.7	1.23	0.0–26.8
HSVE	10	12.7	0.0–57.35	315.5	1.77–552.9	24.84	0.0–57.35
C19 total	18	92.5	0.75–552.4	37.0	0.68–552.1	0.4	0.02–5.09
C19 lowpct	12	51.3	0.75–345.5	7.00	0.68–24.72	0.14	0.02–5.09
C19 highpct	6	174.9	7.1–552.4	96.9	1.54–552.1	0.55	0.02–0.98
<i>IL-16</i>							
NC	11	206.1	165.3–275.8	45.2	39.3–57.6	0.22	0.16–0.3
HSVE	5	253.2	209.8–316.6	115.7	73.8–18.8	0.46	0.31–0.53
C19 total	18	358.9	109.7–775.8	53.3	44.7–74.8	0.15	0.09–0.52
C19 lowpct	12	295.0	109.7–521.2	52.4	44.7–67.2	0.18	0.11–0.52
C19 highpct	6	486.8	226.2–775.8	55.6	43.3–74.8	0.11	0.08–0.19
<i>CXCL10</i>							
NC	11	161.6	91.37–368.4	205.4	89.26–416.1	1.27	0.6–4.04
HSVE	10	256.5	83.37–627.5	894.8	285.9–1087.3	3.49	1.56–13.04
C19 total	18	405.2	32.77–1234.3	226.7	49.06–622.1	0.56	0.08–7.71
C19 lowpct	12	301.8	32.77–765.7	178.0	13.91–622.1	0.59	0.08–7.71
C19 highpct	6	612.1	57.92	324.0	49.83–565.1	0.53	0.2–0.98
<i>PGRN</i>							
NC	22	N.a	N.a	0.9963	0.49–2.09	n.a	n.a
MHSVE	6	N.a	N.a	5.6717	1.04–9.81	n.a	n.a
C19 total	23	N.a	N.a	1.675	0.67–3.04	n.a	n.a
C19 lowpct	13	N.a	N.a	1.678	0.67–3.04	n.a	n.a
C19 highpct	10	N.a	N.a	1.671	0.75–2.22	n.a	n.a

IL-6 = interleukin-6, IL-16 = interleukin-16, CXCL10 = C-X-C motif chemokine 10; n.a. = not available, PGRN = progranulin. NC = non-inflammatory, non-neurodegenerative controls

contactin-associated protein 2 (Caspr2)-IgG were found at a very low titer (1:32) and very low serum IgG antibodies against glycine receptors (1:10). None of these neuronal antibody positive patients had neurological symptoms typically seen in patients with Caspr2- or glycine receptor-related autoimmunity and no confirmatory tests were performed. One patient with upbeat nystagmus after resuscitation had reportedly a 1:100 titer of NMDA receptor IgG antibodies in the serum. CSF was negative for NMDAR antibodies, which is atypical for NMDAR encephalitis and no corresponding IgG binding pattern on native primate hippocampus and cerebellum sections was found. This patient died from hypoxic encephalopathy. Another patient with myoclonia without signs of epilepsy on EEG was positive for serum anti-Yo IgG antibodies in an immunoblot assay at a titer of 1:100 but the result could not be confirmed in by immunohistochemistry, suggesting a false-positive result. Confirmatory testing employing of a CDR2/CDR2L-specific cell-based assay was not performed. At autopsy,

histopathology revealed no signs of cerebellar pathology including normal Purkinje cells.

Cerebrospinal fluid/serum pairs from 16/32 patients were screened on native primate hippocampus and rat cerebellum tissue without any pathological results (see Additional file 1: Table S2). Thus, no pathological autoantibody results could be seen except in one out of 32 + 32 samples.

#### CSF RNA sequencing reveals distinct RNA profiles in COVID-19

RNA profiling of the CSF has been performed to assess another stage of possible neuroinflammatory response. We mapped the reads in the data analysis of RNA sequencing in an exploratory study to both back-splicing-junctions (BSJ) to quantify circular RNAs (circRNAs) and to the linear RNA database to quantify the linear RNAs. In the PCA plot, CSF from patients with severe COVID-19 ( $n = 5$ ) had a distinct linear RNA profile (Fig. 4A) and

**Table 4** Mann–Whitney U-test on IL-6, IL-16, CXCL10

	Progranulin	IL6	IL16	CXCL10
CSF				
NC vs C19 total	<0.001	0.4	<0.001	0.76
NC vs C19 low pct	<0.001	0.09	<0.001	0.65
NC vs C19 high pct	<0.001	0.17	<0.001	0.2
C19 low pct vs C19 high pct	0.98	0.17	0.49	0.1866
Serum				
NC vs C19 total	n.a	0.07	<0.001	<0.001
NC vs C19 low pct	n.a	0.13	<0.001	0.12
NC vs C19 high pct	n.a	<0.001	<0.001	<0.001
C19 low pct vs C19 high pct		0.12	<0.001	0.09
CSF/serum ratio				
NC vs C19 total	n.a	0.12	0.18	0.56
NC vs C19 low pct	n.a	0.25	0.62	0.92
NC vs C19 high pct	n.a	0.27	<0.001	<0.001
C19 low pct vs C19 high pct		0.23	0.08	0.37

Note that progranulin is also synthesized outside the CNS and therefore serum values and ratios were not calculated. *n.a.* = not available. NC = non-inflammatory, non-neurodegenerative controls

a different circRNA profile (Additional file 1: Figure S2A) compared to healthy controls ( $n=4$ ) and neurological diseases ( $n=8$ ). We performed a differential expression analysis on the circRNAs and linear RNAs, and the RNAs were considered to be differentially expressed with  $FDR < 0.05$ . There were two circRNAs (circ\_00022\_SMC1A and circ\_00007\_MAN1A2) downregulated in COVID-19 CSF (Additional file 1: Figure S2B, C).

In the linear RNA profiling data set, 169 linear RNAs were up-regulated and 56 were down-regulated in COVID-19 CSF compared to the CSF of ND patients, while 99 linear RNAs were up-regulated and 31 were down-regulated in COVID-19 CSF compared to healthy controls (Fig. 4B, C, D). There were 73 linear RNAs up-regulated and 28 linear RNAs down-regulated in COVID-19 CSF compared to the CSF from both ND patients and healthy controls (Fig. 4D) and the 101 RNAs were subjected to the enrichment analysis. The enrichment analysis of the SARS-CoV-2 down-regulated genes show the top enriched items, while the enrichment analysis of the down-regulated genes showed that both SARS-CoV-2 up- and down-regulated genes were enriched (Additional file 1: Figure S3). The compartment enrichment analysis of the up-regulated genes showed that synapse and neuron-relevant items were top enriched, while the compartment enrichment analysis of the down-regulated genes showed the extracellular

vesicle-relevant items were top enriched (Additional file 1: Figure S3).

## Discussion

Our results paint the picture of the brain reacting to the inflammatory tidal wave unleashed by COVID-19. Proteomics revealed an almost similar CSF protein profile in COVID-19 patients compared to patients with HSVE, both in patients with and without bacterial superinfection. Although the protein expression in general is much stronger in the HSVE group than in the COVID-19 patients. Proteins of the immunological pathway such as Progranulin are also slightly but still significantly elevated in the CSF of COVID-19 patients but not antibodies against neuronal targets. COVID-19 seems to increase the number of pathways initiated compared to HSVE pointing at a broader activation due to COVID-19.

The observed changes were much less pronounced in COVID-19 than in HSVE. Of note, the proteins found to be elevated in COVID-19 were mainly of extrathecal origin as indicated by normal CSF/serum ratios, reflecting probably both the pronounced systemic inflammatory reaction in COVID-19 and the high frequency of minor blood–CSF barrier disruption as previously reported in patients with COVID-19. Moreover, some of the proteins found to be elevated in the CSF, such as LRG1 and the proteins of the Serpin family, are not known to be produced within the CNS but were previously found, including in proteomic studies, in the plasma of patients with COVID-19, further suggesting diffusion from the blood into the CSF (22, 38).

The presence of bacterial superinfection had not been taken into account in previous studies on the neuroimmunological impact of COVID-19. Bacterial superinfection (BSI) was associated with significantly increased levels of the inflammation-related proteins studied and did affect the protein pattern itself with a few more proteins in the COVID-19<sub>highpct</sub> group. Only in case the proteomics results are rephrased to REACTOME phrases the difference in intensity remain with a predominance on HSVE but the activated pathways connected to the protein pattern show a predominance in COVID-19 (Fig. 1A vs 1B). The role of the three proteins C4a, CD14 and NRCAM driving the difference between BSI remains elusive with in the one hand inflammatory proteins making the difference being well in line (Additional file 1: Figure S1). On the other hand, no connection between these proteins is known. More experiments are needed here to understand this result.

Results from the array pointed to elevated serum concentrations of integrins such as ICAM1 or hemostasis-related proteins such as SerpinE1 in the serum of

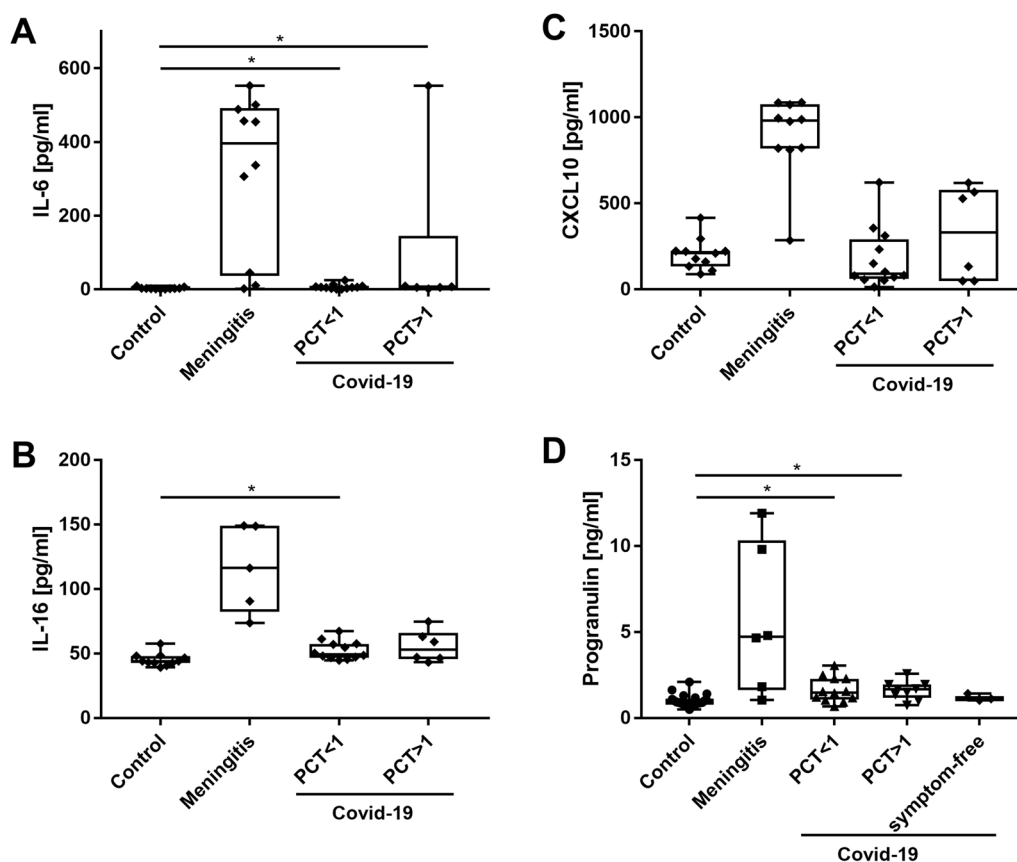


**Fig. 3** Cytokine and progranulin levels in the CSF. Please note that HSVE levels were not part of the statistical analysis due to the high levels of cytokines. **A** Interleukin-6 (IL-6). **B** Interleukin-16 (IL-16). **C** CXCL10. **D** Progranulin levels. \* $p < 0.05$ ; \*\* $p < 0.01$

COVID-19 patients. Our study reaffirms previous studies reporting increased IL-6, CXCL10 and IL-16 serum levels in patients with COVID-19 with BSI being a major bias (13, 39).

Progranulin levels are significantly increased in the CSF of symptomatic and asymptomatic COVID-19 patients, in patients with and without bacterial superinfection and both in a patient with mild and severe symptoms. This independence of the WHO stage of COVID-19 may give a hint towards a general activation of this protein in COVID-19. Progranulin is not known as a marker for neuronal death but for neuroprotection (40–42). One hypothesis for the increase of progranulin is that the brain is reactively increasing its neuroprotective and anti-inflammatory stockpile. Thus, progranulin in the CSF would be a result of microglial and neuronal activation, which has in fact been shown in several neuropathological post-mortem and animal COVID-19 studies (7–9). Progranulin in the rodent brain is most strongly expressed in the olfactory and temporal regions and Sars-CoV2 has been proven to infiltrate this system in the animal model. Another possible explanation could

be that progranulin is maybe released during the infiltration of these regions (8, 21, 37). The known COVID-19 symptoms of dysgeusia and dysosmia are not depending on disease severity. This supports our progranulin data because progranulin levels were also independent from COVID-19 disease severity in our cohort. The CSF/serum ratios are not reasonable here because progranulin is produced also outside the CNS in large amounts (17, 18).

Thus, high progranulin CSF levels and low cytokine CSF/serum ratios together may point at a brain in a defensive state against the inflammatory storm coming from the blood. The specific protein results on their own may explain the normal CSF routine parameter measured here and in other studies (13, 43, 44) going along with neurological symptoms as these small concentrations are possibly able to initiate a weak response of the brain.

Normal CSF routine parameters have been seen before also in symptomatic antibody-associated autoimmune encephalitis (45–47). Extensive screening for anti-neural antibodies including on native neuronal tissue did not reveal any pathological titers of known antibodies nor did



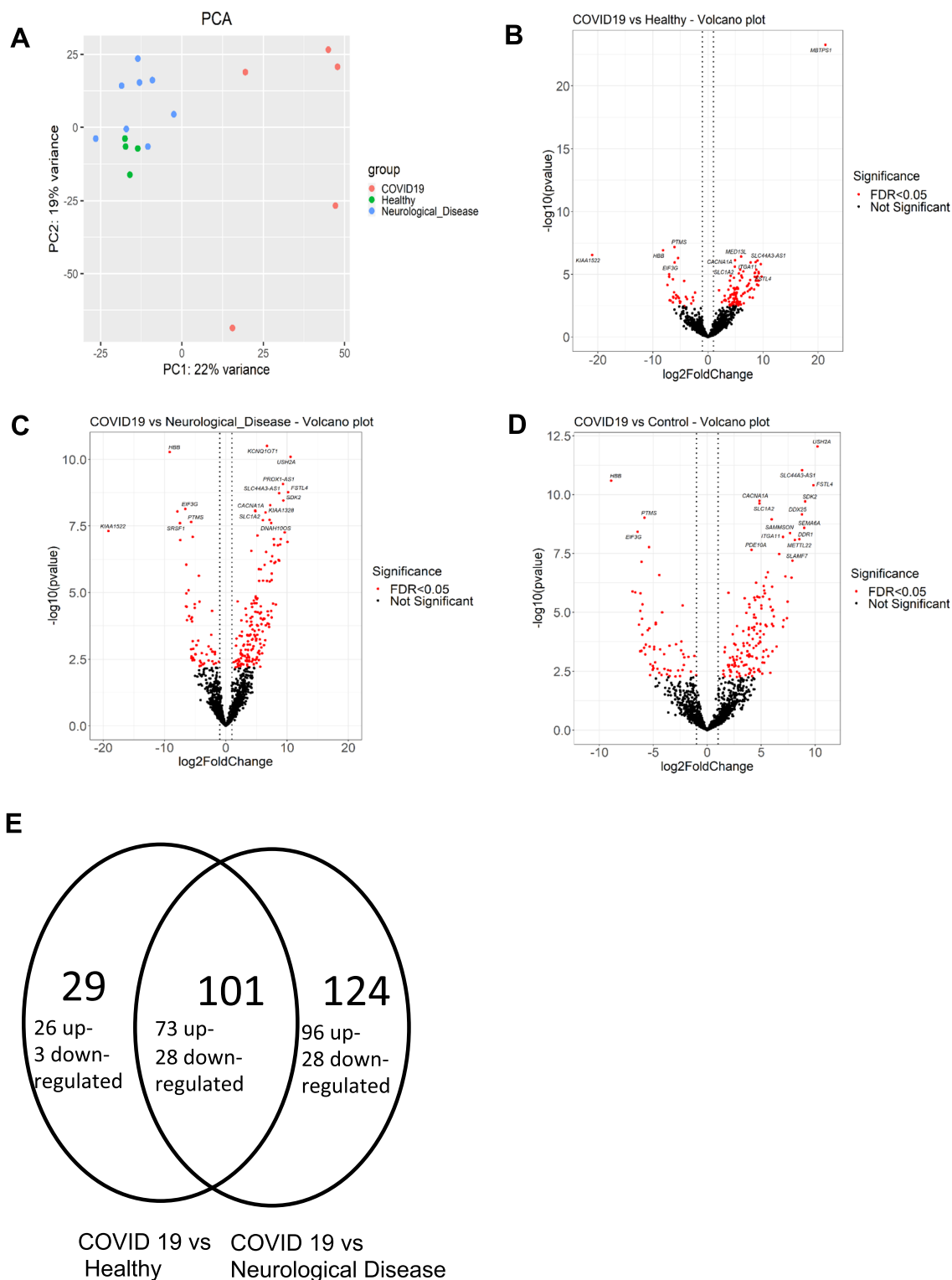


**Fig. 4** Linear RNA data analysis. **A** Principal component analysis (PCA) of linear RNA profile in the CSF of COVID-19 patients, healthy controls and patients with neurological disease (AD and MS). Differential expression analysis of linear RNAs in **B** CSF of COVID-19 patients and healthy controls, **C** CSF of COVID-19 patients and patients with neurological disease and **D** CSF of COVID-19 patients and all controls. Red dots: FDR < 0.05

it reveal any novel, unknown antibody reactivities. Our cohort did comprise some patients with focal neurological symptoms such as oculomotor palsy but most of them had unspecific neurological symptoms such as encephalopathy that might in total lower the risk for antibody detection in our cohort (see Additional file 1: Table S2). Still, the absence of anti-neural autoantibodies at clinically relevant titers in 32 patients argues against a major role of antibody-mediated mechanisms in the pathophysiology of COVID-19 with neurological symptoms as seen before (13).

Transcriptomics seems to reveal a heterogenous picture pointing at an increased RNA activity in neurons and synapses. Given previous evidence suggesting that SARS-CoV-2 infection of the CNS is very rare if it occurs at all, it seems unlikely that the altered linear RNA profile in the CSF of patients with COVID-19 and neurological involvement compared to healthy controls and patients with other neurological diseases observed in our study reflect direct SARS-CoV-2-mediated neural damage. Instead, these results show rather indirect, systemic effects in the brain, e.g., diffusion of mediators of inflammation from the peripheral circulation into the CNS, either passively or through a leaky blood brain barrier, hypoxia and/or brain endothelial cell damage. In the enrichment analysis of up-regulated genes in COVID-19 CSF, the significantly enriched items are the down-regulated genes by SARS-CoV-2 in cells or tissues, which indicated that one COVID-19 pathomechanism may be force the neurons to secrete RNAs. Hypothetically, the deregulation of RNAs and the result of the enrichment analysis indicated that SARS-CoV-2 infection can induce the secretion of RNAs from synapse and neuron into CSF. These RNAs may be packed into extracellular vesicles, which caused the down regulation of the standard RNA packing in these vesicles. Further analysis and validation are needed to investigate the reasons for the change of CSF RNA profile after SARS-CoV-2 infection.

Among the down-regulated linear RNAs in COVID-19 CSF in our study, *HBB* (*Hemoglobin subunit beta*) was not detectable in every COVID-19 CSF samples, while it was expressed in all other CSF samples. Blood contamination as a source of *HBB* seems to be very unlikely. Maybe this finding is due to the previously reported SARS-CoV-2 attack on the heme on the 1-B chain of hemoglobin eventually causing a lower amount of hemoglobin (48). Hypothetically, disruption of this pathway would lead to a reactive increase of HBB resulting in downregulation. Also, in our enrichment analysis, the down-regulated genes were found to be associated with extracellular vesicles, which suggests that COVID-19 may affect the RNA profile of extracellular vesicles derived from the brain.

Now that the new Omicron variant is epidemic, significantly fewer infections with accompanying neurologic symptoms are reported. This is consistent with our finding that the intensity of inflammation is a critical component in the incidence of neurologic symptoms.

Limitations of the study are the different sample sizes used per approach, which is due to different volume requirements for different measurements on the one hand and restricted CSF volumes per patient. Another limitation is the different handling times per sample which could result into volatile substances being no longer detectable.

## Conclusion

In conclusion, our multi-omics and protein analysis approach suggest that although COVID-19 is not an active neuroinflammatory disease, it does affect the brain indirectly through the activated inflammatory pathways outside the brain. Also, further studies need to take into account superinfections and other concomitant diseases enhancing the immunological pathways and biasing the results. The role of progranulin and interleukin-16 in COVID-19 deserves more attention in the future.

## Abbreviations

AD	Alzheimer's dementia
ARHGAP26	Rho GTPase-activating protein 26
AMPA	Amino-3-hydroxy-5 methyl-4-isoxazolepropionic acid receptor
BSI	Bacterial superinfection
Caspr2	Contactin-associated protein 2
CBA	Culture based assay
CNS	Central nervous system
circRNA	Circular RNA
COVID-19	Coronavirus disease 2019
CV2/CRMP5	Cytoplasmic protein 5
CXCL-10	C-X-C motif chemokine 10
DPPX	Dipeptidyl-peptidase-like protein-6
ELISA	Enzyme-linked immunofluorescence assay
FDR	False discovery rate
GABAaR	Gamma-amino-butyrata-a-receptor
GABA <sub>b</sub> R	Gamma-amino-butyrata-b-receptor
GAD-65	Glutamic acid decarboxylase 65
HSVE	Herpes-simplex virus meningoencephalitis
IAA	Indole-3-acetic acid
IL-6	Interleukin-6
ITPR1/anti-Sj	Inositol 1,4,5-trisphosphate receptor type 1
LGI-1	Leucine-rich glioma inactivated protein 1
M	Molar
mGluR1	Metabotropic glutamate receptor 1
mGluR5	Metabotropic glutamate receptor 5
MOG	Myelin-oligodendrocyte glycoprotein
NMDAR	N-Methyl-D-aspartate receptor
PCA	Principal component analysis
PCT	Procalcitonin
PGRN	Progranulin
ROI	Region of interest
RT	Room temperature
SARS-CoV2	Severe acute respiratory syndrome coronavirus 2
Tr/DNER	Delta/notch-like epidermal growth factor

## Supplementary Information

The online version contains supplementary material available at <https://doi.org/10.1186/s12974-023-02711-2>.

**Additional file 1.** Supplementary tables and figures.

### Acknowledgements

The authors are grateful to Kerstin Kaiser und Jeanette Witzke, Neurochemistry Laboratory, Department of Neurology, University Hospital Magdeburg, Magdeburg, Germany.

### Author contributions

Dirk Reinhold, Vadim Farztdinov and Yan Yan share the first authorship. Co-authorships of the first authors: everyone of the first authors had a different part of the experiments: proteins, proteomics and RNAs. Conceptualization: DR, VF, YY, KL, HR, JK, MM, FH, PK. Methodology: DR, KG, AG, VF, MR, MM, YY, MV, JK, SS, HR, FH, PK. Investigation: DR, KG, VF, MM, YY, MV, JK, SS, HR, CO, KR, PS, FK, CM, HS, JK, SV, FHP, BT, WS, PK. Visualization: DR, KG, AG, VF, MM, YY, VM, PK. Funding acquisition: HR, ED, FH, JK, MR. Project administration: HR, CM, HS, JK, FHP, PK. Supervision: FH, MR, LES, PK. Writing—original draft: PK, DR, VF, YY, MM. Writing—review and editing: PK, DR, VF, YY, MM, ME, SJ, KR, SS, JK. All authors read and approved the final manuscript.

### Funding

Open Access funding enabled and organized by Projekt DEAL. This manuscript is funded by the publication funds of the Charité Universitätsmedizin Berlin, Germany.

### Availability of data and materials

All data, code, and materials used in the analysis are available per email request to the corresponding author.

### Declarations

#### Ethics approval and consent to participate

This study has been approved by the ethics committee of the Charité Universitätsmedizin Berlin (EA176\_20). Every patient gave written and informed consent.

#### Consent for publication

Not applicable.

#### Competing interests

Authors declare that they have no competing interests concerning the issues in this manuscript.

#### Author details

<sup>1</sup>Institute of Molecular and Clinical Immunology, Medical Faculty, Otto-Von-Guericke-University, Magdeburg, Germany. <sup>2</sup>Health Campus Immunology, Infectiology and Inflammation (GC-I3), Medical Faculty, Otto-Von-Guericke-University, Magdeburg, Germany. <sup>3</sup>Core Facility, High-Throughput Mass Spectrometry, Charité, Universitätsmedizin Berlin, corporate member of Freie Universität Berlin and Humboldt-Universität Zu Berlin, Berlin, Germany. <sup>4</sup>Interdisciplinary Nanoscience Center, Aarhus University, 8000 Aarhus C, Denmark. <sup>5</sup>Omiics ApS, 8200 Aarhus N, Denmark. <sup>6</sup>Labor Berlin Charité Vivantes GmbH, 13353 Berlin, Germany. <sup>7</sup>Department of Neurology, Charité, Universitätsmedizin Berlin, corporate member of Freie Universität Berlin and Humboldt-Universität Zu Berlin, Campus Benjamin Franklin, Hindenburgdamm 30, 12200 Berlin, Germany. <sup>8</sup>German Center for Neurodegenerative Diseases (DZNE) in Berlin, 10117 Berlin, Germany. <sup>9</sup>German Center for Neurodegenerative Diseases (DZNE) in Magdeburg, 39120 Magdeburg, Germany. <sup>10</sup>Department of Neurology, University Hospital Magdeburg, Otto-Von-Guericke University, 39120 Magdeburg, Germany. <sup>11</sup>Clinical-Immunological Laboratory Prof. Dr. Stöcker, 23627 Groß Grönau, Germany. <sup>12</sup>Department of Infectious Diseases and Respiratory Medicine, German Center for Lung Research (DZL), Charité, Universitätsmedizin Berlin, corporate member of Freie Universität Berlin and Humboldt-Universität Zu Berlin, Berlin, Germany. <sup>13</sup>Department of Neuropathology, Charité, Universitätsmedizin Berlin, corporate member

of Freie Universität Berlin and Humboldt-Universität Zu Berlin, Charitéplatz 1, 10117 Berlin, Germany. <sup>14</sup>Molecular Neuroimmunology Group, Department of Neurology, University of Heidelberg, Heidelberg, Germany. <sup>15</sup>Institute for Biochemistry, Charité Universitätsmedizin Berlin, Berlin, Germany.

Received: 2 July 2022 Accepted: 30 January 2023

Published online: 09 February 2023

### References

- Helms J, Kremer S, Merdji H, Clere-Jehl R, Schenck M, Kummerlen C, et al. Neurologic features in severe SARS-CoV-2 infection. *N Engl J Med*. 2020;382(23):2268–70.
- Frontera JA, Sabadia S, Lalchan R, Fang T, Flusty B, Millar-Verneti P, et al. A prospective study of neurologic disorders in hospitalized COVID-19 patients in New York City. *Neurology*. 2020. <https://doi.org/10.1212/WNL.000000000010979>.
- Paterson RW, Brown RL, Benjamin L, Nortley R, Wiethoff S, Bharucha T, et al. The emerging spectrum of COVID-19 neurology: clinical, radiological and laboratory findings. *Brain*. 2020;143(10):3104–20.
- Patrick E, Rajagopal S, Wong HKA, McCabe C, Xu J, Tang A, et al. Dissecting the role of non-coding RNAs in the accumulation of amyloid and tau neuropathologies in Alzheimer's disease. *Mol Neurodegener*. 2017;12(1):1–13.
- Yang AC, Kern F, Losada PM, Agam MR, Maat CA, Schmartz GP, et al. Dysregulation of brain and choroid plexus cell types in severe COVID-19. *Nature* [Internet]. 2021;595(7868):565–71. <https://doi.org/10.1038/s41586-021-03710-0>.
- Iadecola C, Anrather J, Kamel H. Effects of COVID-19 on the nervous system. *Cell* [Internet]. 2020;183(1):16–27. <https://doi.org/10.1016/j.cell.2020.08.028>.
- Fernández-Castañeda A, Lu P, Geraghty AC, Song E, Lee M-H, Wood J, et al. Mild respiratory SARS-CoV-2 infection can cause multi-lineage cellular dysregulation and myelin loss in the brain. *bioRxiv* [Internet]. 2022;2022.01.07.475453. Available from: <http://biorxiv.org/content/early/2022/01/10/2022.01.07.475453.abstract>.
- Meinhardt J, Radke J, Dittmayer C, Franz J, Thomas C, Mothes R, et al. Olfactory transmucosal SARS-CoV-2 invasion as a port of central nervous system entry in individuals with COVID-19. *Nat Neurosci*. 2020;11:1200.
- Matschke J, Lütthgehetmann M, Hagem C. Neuropathology of patients with COVID-19 in Germany: a post-mortem case series. *Lancet Neurol*. 2020;19(January):919–29.
- Deigendesch N, Sironi L, Kutza M, Wischnewski S, Fuchs V, Hench J, et al. Correlates of critical illness-related encephalopathy predominate postmortem COVID-19 neuropathology. *Acta Neuropathol* [Internet]. 2020;140(4):583–6. <https://doi.org/10.1007/s00401-020-02213-y>.
- Schwabenland M, Salié H, Tanevski J, Killmer S, Lago MS, Schlaak AE, et al. Deep spatial profiling of human COVID-19 brains reveals neuroinflammation with distinct microanatomical microglia-T-cell interactions. *Immunity* [Internet]. 2021;54(7):1594–610. <https://doi.org/10.1016/j.immuni.2021.06.002>.
- Virhammar J, Nääs A, Fällmar D, Cunningham JL, Klang A, Ashton NJ, et al. Biomarkers for central nervous system injury in cerebrospinal fluid are elevated in COVID-19 and associated with neurological symptoms and disease severity. *Eur J Neurol*. 2021;(November 2020):1–8.
- Jarius S, Pache F, Körtvelyessy P, Jelčić I, Stettner M, Franciotta D. Cerebrospinal fluid findings in COVID-19: a multicenter study of 150 lumbar punctures in 127 patients. *J Neuroinflammation* [Internet]. 2022. <https://doi.org/10.1186/s12974-021-02339-0>.
- Neumann B, Schmidbauer ML, Dimitriadis K, Otto S, Knier B, Niesen W-D, et al. Cerebrospinal fluid findings in COVID-19 patients with neurological symptoms. *J Neurol Sci* [Internet]. 2020. <https://doi.org/10.1016/j.jns.2020.117090>.
- Miller EH, Namale VS, Kim C, Dugue R, Waldrop G, Ciryam P, et al. Cerebrospinal analysis in patients with COVID-19. *Open Forum Infect Dis* [Internet]. 2020;7(11):ofaa501. <https://doi.org/10.1093/ofid/ofaa501>.
- Körtvelyessy P, Gohl A, Guttek K, Schraven B, Prüss H, Reinhold D. Serum and CSF cytokine levels mirror different neuroimmunological mechanisms in patients with LGI1 and Caspr2 encephalitis. *Cytokine*. 2020;135(Nov):15526.

17. Nicholson AM, Finch NCA, Thomas CS, Wojtas A, Rutherford NJ, Mielke MM, et al. Progranulin protein levels are differently regulated in plasma and CSF. *Neurology*. 2014;82(21):1871–8.
18. Wilke C, Gillardon F, Deuschle C, Dubois E, Hobert M, Müller vom Hagen J, et al. Serum levels of progranulin do not reflect cerebrospinal fluid levels in neurodegenerative disease. *Curr Alzheimer Res*. 2016;13(6):654–62.
19. Wilke C, Gillardon F, Deuschle C, Hobert MA, Jansen IE, Metzger FG, et al. Cerebrospinal fluid progranulin, but not serum progranulin, is reduced in GRN-negative frontotemporal dementia. *Neurodegener Dis*. 2017;17(2–3):83–8.
20. Körtvélyessy P, Prüss H, Thurner L, Maetzler W, Vittore-Welliong D, Schultze-Amberger J, et al. Biomarkers of neurodegeneration in autoimmune-mediated encephalitis. *Front Neurol*. 2018;9:668.
21. Körtvélyessy P, Gukasjan A, Sweeney-Reed CM, Heinze HJ, Thurner L, Bittner DM. Progranulin and amyloid- $\beta$  levels: relationship to neuropsychology in frontotemporal and Alzheimer's disease. *J Alzheimer's Dis*. 2015;
22. Messner CB, Demichev V, Wendisch D, Michalick L, White M, Freiwald A, et al. Ultra-high-throughput clinical proteomics reveals classifiers of COVID-19 infection. *Cell Syst*. 2020;11(1):11–24.e4.
23. Messner CB, Demichev V, Bloomfield N, Yu JSL, White M, Kreidl M, et al. Ultra-fast proteomics with Scanning SWATH. *Nat Biotechnol* [Internet]. 2021;39(7):846–54. <https://doi.org/10.1038/s41587-021-00860-4>.
24. Demichev V, Messner CB, Vernardis SI, Lilley KS, Ralser M. DIA-NN: neural networks and interference correction enable deep proteome coverage in high throughput. *Nat Methods* [Internet]. 2020;17(1):41–4. <https://doi.org/10.1038/s41592-019-0638-x>.
25. Bian Y, Zheng R, Bayer FP, Wong C, Chang Y-C, Meng C, et al. Robust, reproducible and quantitative analysis of thousands of proteomes by micro-flow LC-MS/MS. *Nat Commun* [Internet]. 2020;11(1):157. <https://doi.org/10.1038/s41467-019-13973-x>.
26. Consortium TU. UniProt: a worldwide hub of protein knowledge. *Nucleic Acids Res* [Internet]. 2019;47(D1):D506–15. <https://doi.org/10.1093/nar/gky1049>.
27. Josse J, Husson F. missMDA: A Package for Handling Missing Values in Multivariate Data Analysis. *J Stat Softw* [Internet]. 2016;70(1 SE-Articles):1–31. Available from: <https://www.jstatsoft.org/index.php/jss/article/view/v070i01>.
28. Ritchie ME, Phipson B, Wu D, Hu Y, Law CW, Shi W, et al. limma powers differential expression analyses for RNA-sequencing and microarray studies. *Nucleic Acids Res* [Internet]. 2015;43(7):e47–e47. <https://doi.org/10.1093/nar/gkv007>.
29. Bolstad BM, Irizarry RA, Åstrand M, Speed TP. A comparison of normalization methods for high density oligonucleotide array data based on variance and bias. *Bioinformatics* [Internet]. 2003;19(2):185–93. <https://doi.org/10.1093/bioinformatics/19.2.185>.
30. Ballman KV, Grill DE, Oberg AL, Therneau TM. Faster cyclic loess: normalizing RNA arrays via linear models. *Bioinformatics* [Internet]. 2004;20(16):2778–86. <https://doi.org/10.1093/bioinformatics/bth327>.
31. Cox J, Hein MY, Lubner CA, Paron I, Nagaraj N, Mann M. Accurate proteome-wide label-free quantification by delayed normalization and maximal peptide ratio extraction, termed MaxLFQ. *Mol Cell Proteomics* [Internet]. 2014;13(9):2513–26.
32. Pham TV, Henneman AA, Jimenez CR. iq: an R package to estimate relative protein abundances from ion quantification in DIA-MS-based proteomics. *Bioinformatics* [Internet]. 2020;36(8):2611–3.
33. Benjamini Y, Hochberg Y. Controlling the false discovery rate: a practical and powerful approach to multiple testing. *J R Stat Soc Ser B* [Internet]. 1995;57(1):289–300.
34. Xie Z, Bailey A, Kuleshov MV, Clarke DJB, Evangelista JE, Jenkins SL, et al. Gene set knowledge discovery with enrichr. *Curr Protoc*. 2021;1(3): e90.
35. Kao AW, McKay A, Singh PP, Brunet A, Huang EJ. Progranulin, lysosomal regulation and neurodegenerative disease. *Nat Rev Neurosci*. 2017;18:325–33.
36. De Muynck L, Van Damme P. Cellular effects of progranulin in health and disease. *J Mol Neurosci*. 2011; 549–60.
37. Daniel R, He Z, Carmichael KP, Halper J, Bateman A. Cellular localization of gene expression for progranulin. *J Histochem Cytochem* [Internet]. 2000;48(7):999–1009.
38. Pretorius E, Vlok M, Venter C, Bezuidenhout JA, Laubscher GJ, Steenkamp J, et al. Persistent clotting protein pathology in Long COVID/Post-Acute Sequelae of COVID-19 (PASC) is accompanied by increased levels of antiplasmin. *Cardiovasc Diabetol* [Internet]. 2021;20(1):1–18. <https://doi.org/10.1186/s12933-021-01359-7>.
39. Jøntvedt Jørgensen M, Holter JC, Christensen EE, Schjalm C, Tonby K, Pischke SE, et al. Increased interleukin-6 and macrophage chemoattractant protein-1 are associated with respiratory failure in COVID-19. *Sci Rep* [Internet]. 2020;10(1):21697. <https://doi.org/10.1038/s41598-020-78710-7>.
40. Ma Y, Matsuwaki T, Yamanouchi K, Nishihara M. Progranulin protects hippocampal neurogenesis via suppression of neuroinflammatory responses under acute immune stress. *Mol Neurobiol* [Internet]. 2017;54(5):3717–28. <https://doi.org/10.1007/s12035-016-9939-6>.
41. Huchtemann T, Körtvélyessy P, Feistner H, Heinze HJ, Bittner D. Progranulin levels in status epilepticus as a marker of neuronal recovery and neuroprotection. *Epilepsy Behav*. 2015;49:170–2.
42. Chitrathuthu BP, Bennett HPJ, Bateman A. Progranulin: a new avenue towards the understanding and treatment of neurodegenerative disease. *Brain*. 2017;140:3081–104.
43. Lersy F, Benotmane I, Helms J, Collange O, Schenck M, Brisset JC, et al. Cerebrospinal fluid features in patients with coronavirus disease 2019 and neurological manifestations: correlation with brain magnetic resonance imaging findings in 58 patients. *J Infect Dis*. 2021;223(4):600–9.
44. Lewis A, Frontera J, Placantonakis DG, Lighter J. Cerebrospinal Fluid in COVID-19 a systematic review of the literature. *J Neurol Sci*. 2021;421(January): 117316.
45. Gresa-Arribas N, Titulaer MJ, Torrents A, Aguilar E, McCracken L, Leypoldt F, et al. Antibody titres at diagnosis and during follow-up of anti-NMDA receptor encephalitis: a retrospective study. *Lancet Neurol* [Internet]. 2014;13(2):167–77. [https://doi.org/10.1016/S1474-4422\(13\)70282-5](https://doi.org/10.1016/S1474-4422(13)70282-5).
46. Van Sonderen A, Ariño H, Petit-Pedrol M, Leypoldt F, Körtvélyessy P, Wandinger KP, et al. The clinical spectrum of Caspr2 antibody-associated disease. *Neurology*. 2016;87(5):521–8.
47. Arino H, Armangue T, Petit-Pedrol M, Sabater L, Martínez-Hernández E, Hara M, et al. Anti-LGI1-associated cognitive impairment presentation and long-term outcome. *Neurology*. 2016;87(8):1–8.
48. Wenzhong L, Hualan L. COVID-19: attacks the 1-beta chain of hemoglobin and captures the porphyrin to inhibit human heme metabolism. *ChemRxiv*. 2020;4:1–38.

## Publisher's Note

Springer Nature remains neutral with regard to jurisdictional claims in published maps and institutional affiliations.

Ready to submit your research? Choose BMC and benefit from:

- fast, convenient online submission
- thorough peer review by experienced researchers in your field
- rapid publication on acceptance
- support for research data, including large and complex data types
- gold Open Access which fosters wider collaboration and increased citations
- maximum visibility for your research: over 100M website views per year

At BMC, research is always in progress.

Learn more [biomedcentral.com/submissions](https://biomedcentral.com/submissions)

